



# Systematically investigating the pharmacological mechanism of Guizhi Gancao decoction in promoting thermogenesis during cold exposure by integrating HPLC-Q-TOF/MS analysis and network pharmacology



Zexu Shen<sup>a,1</sup>, Xiang Li<sup>a,1</sup>, Chenghui Yan<sup>b</sup>, Tianshu Ren<sup>a</sup>, Bo Xing<sup>a</sup>, Yingying Qu<sup>a</sup>, Dong Yao<sup>a</sup>, Zihua Xu<sup>a,\*,2</sup>, Yaling Han<sup>b,2,\*</sup>, Qingchun Zhao<sup>a,\*,2</sup>

<sup>a</sup> Department of Clinical Pharmacy, General Hospital of Northern Theatre Command, Shenyang 110840, China

<sup>b</sup> Department of Cardiology, General Hospital of Northern Theatre Command, Shenyang 110840, China

## ARTICLE INFO

### Keywords:

Guizhi Gancao Decoction  
 Anti-cold activity  
 Brown adipose tissue  
 PPAR $\gamma$  pathway  
 Network pharmacology  
 Thermogenesis

## ABSTRACT

**Background:** Guizhi Gancao Decoction (GGD), a classic formula in Traditional Chinese Medicine (TCM), is composed of *Ramulus Cinnamomi* (RC) and *Radix Glycyrrhizae* (RG). It is traditionally used to restore heart Yang and promote Qi transformation. However, its anti-cold effects, underlying mechanisms, and primary active components remain to be fully elucidated.

**Objective:** To investigate the anti-cold activity of GGD, identify its primary active components, and further explore its underlying mechanisms.

**Methods:** Mice were randomized into six groups (n = 10): control (no cold exposure), model (cold exposure), Miglitol (50 mg/kg, cold exposure), and three GGD groups (1, 2, 4 g/kg, cold exposure). After 21 days of treatment, body temperature and athletic performance were assessed. The main components of GGD were identified using HPLC-Q-TOF-MS, and network pharmacology was employed to analyze key compounds, targets, and biological processes. The pivotal signaling pathway was experimentally validated.

**Results:** GGD significantly alleviated hypothermia induced by cold exposure, while reducing total cholesterol, lipid droplets, mitochondrial membrane potential, and Adenosine

Triphosphate (ATP) production in brown adipose tissue (BAT). Additionally, GGD significantly upregulated the expression of Uncoupling protein 1 (UCP1) and its upstream regulator, Peroxisome proliferator-activated receptor  $\gamma$  (PPAR $\gamma$ ).

**Conclusions:** Administration of GGD maintains core body temperature during cold exposure by activating BAT via the PPAR $\gamma$  signaling pathway. The key compounds licochalcone D, hispaglabridin A, and cinnamic acid target PPAR $\gamma$ , UCP1, and Peroxisome proliferator-activated receptor gamma coactivator 1-alpha (PGC1- $\alpha$ ) respectively, regulating fatty acid oxidation and lipid metabolism. These compounds contribute to enhanced thermogenesis via PPAR $\gamma$  pathway. The prescription has the potential to be developed as a medicine for increasing thermogenesis in cold conditions.

## Introduction

Frostbite refers to tissue damage caused by a drop in body or local temperature due to exposure to the cold environments or prolonged low temperatures.<sup>1</sup> It is a common condition among individuals involved in winter military operations, scientific research, mountaineering, and

exploration in alpine regions.<sup>2</sup> The long duration of the disease, complex treatment, and high disability rate make frostbite prevention a critical task.

In mammals, adaptive thermogenesis is regulated by two main mechanisms, shivering and non-shivering thermogenesis (NST).<sup>3</sup> In shivering thermogenesis, temperature-sensitive neurons in the cervical spinal cord respond to cold stimulation causing opposing muscles to

\* Corresponding authors.

E-mail addresses: [xuzihua-668585@163.com](mailto:xuzihua-668585@163.com) (Z. Xu), [lixiangsyphu@126.com](mailto:lixiangsyphu@126.com) (Y. Han), [zhaqingchun1967@163.com](mailto:zhaqingchun1967@163.com) (Q. Zhao).

<sup>1</sup> Zexu Shen and Xiang Li contributed equally to this work and share the first author.

<sup>2</sup> Qingchun Zhao, Yaling Han and Zihua Xu contributed equally to this work and share the Corresponding author

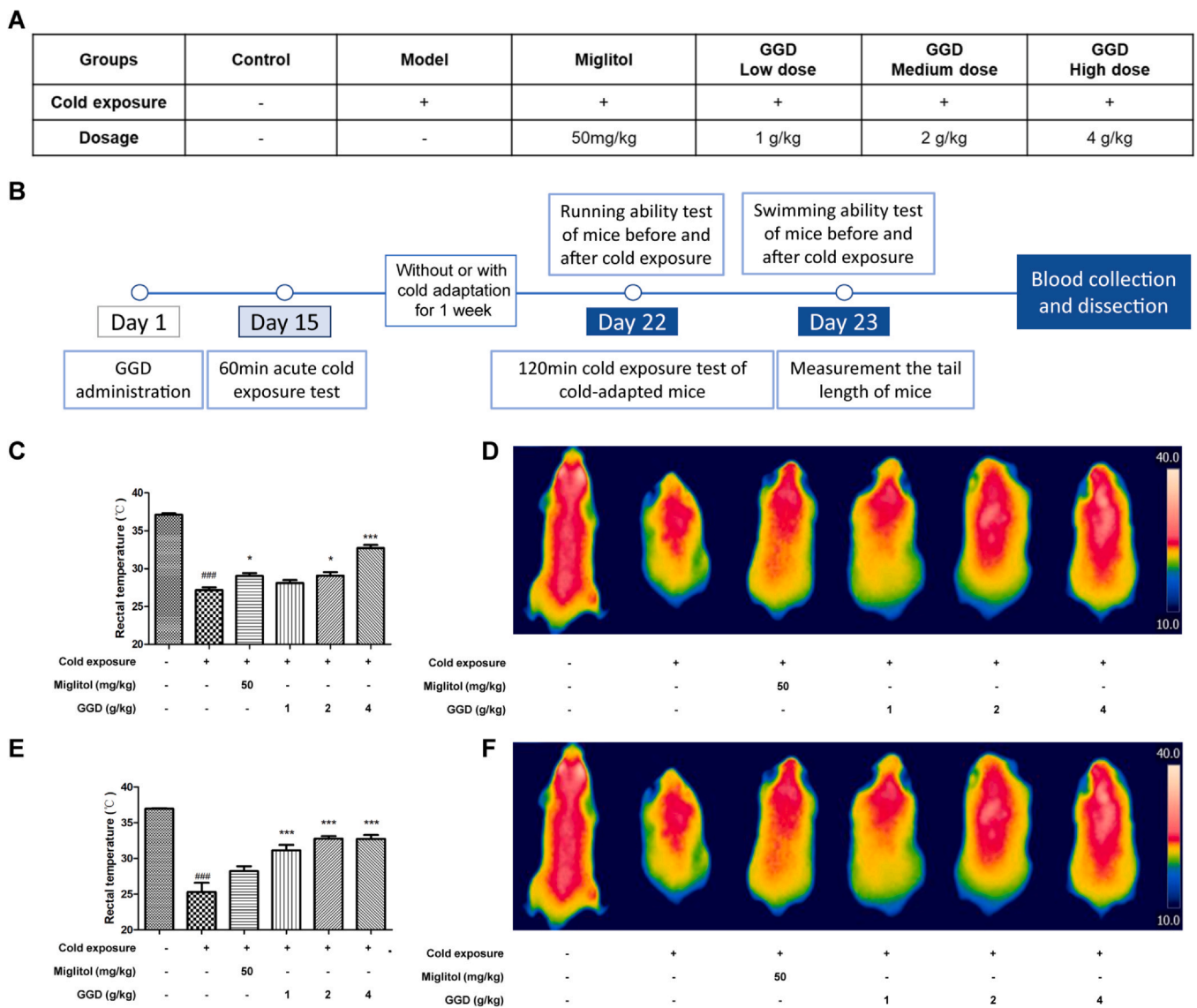


**Fig. 1.** Experimental design and GGD potency in a cold environment. (A, B) Dose and experimental scheme. (C, D) The core body temperature and shell temperature after acute cold exposure in  $-20^{\circ}\text{C}$  for 60 min. (E, F) The core body temperature and shell temperature of cold-adapted mice after cold exposure in  $-20^{\circ}\text{C}$  for 120 min. Data were presented as mean  $\pm$  SEM analyzed by one-way ANOVA ( $n = 10$ ) and Turkey post-tests. \* $p < 0.01$  vs; Model group \*\*\*  $p < 0.001$  vs; Model group, ###  $p < 0.001$  vs. Control group. GGD, Guizhi Gancao Decoction.

contract without load, thereby converting chemical energy into thermal energy without physical exercise. However, shivering can impair movement.<sup>4</sup> In contrast, NST is primarily triggered by a cold sensation from the skin and involves non-muscle contraction, which does not interfere with movement. During acute cold exposure, NST-mediated metabolic activity accounts for approximately one-third of total body heat production, making it a more effective, comfortable, and sustainable thermogenesis mechanism.<sup>3,5</sup>

In the thermogenic organs, Brown adipose tissue (BAT) is a unique type of fat that consumes energy to generate heat, playing a crucial role in NST and resistance to hypothermia in mammals.<sup>6</sup> The biological function of BAT is primarily regulated by the sympathetic nervous system. In the mitochondrial membrane, Uncoupling protein 1 (UCP1) catalyzes  $\text{H}^+$  to return directly to the mitochondrial matrix through specific channels, which dissipates the  $\text{H}^+$  transmembrane potential gradient, reduces the mitochondrial membrane potential, and uncouples oxidation from phosphorylation, ultimately dissipating energy as heat without generating ATP.<sup>7</sup> Miglitol and other diabetes medications have been reported to increase expression in mice fed a high-fat diet.<sup>8,9</sup> In this study, miglitol was used as a positive control to stimulate UCP1 expression.

*Guizhi Gancao decoction* is a well-known classical formula in Traditional Chinese Medicine (TCM) consisting of two medicinal herbs, as recorded in the *Treatise on Febrile Diseases*. The two herbs are *Ramulus Cinnamomi* (RC, *Cinnamomum cassia* (L.) J. Presl, [Lauraceae]) and *Radix Glycyrrhizae* (RG, *Glycyrrhiza glabra* L., [Fabaceae]). According to TCM theory, RC has a sweet and warm property that reinforces heart Yang. Yang-tonifying herbs tend to boost body function possibly through enhancing the mitochondrial oxidative processes,<sup>10</sup> which makes RC the main medicine of this recipe. Qi (vital energy) is regarded as a driving force of biological activities in the human body, including both nutrient substances and organ functions.<sup>11</sup> The RG, as a Qi-tonic herb, acts as the assistant of RC and plays a role in mitochondrial ATP generation.

Cinnamon (*Cinnamomum cassia*) is the dried bark of the Cinnamon tree (*C. cassia*). Its pungent, hot, and sweet properties make it particularly effective for revitalizing the fire element, fostering Yang energy, dispersing chill, and warming meridians.<sup>12</sup> This herb is commonly used to treat cold syndromes. Cinnamaldehyde and cinnamic acid are the primary active components of cinnamon. Recent studies have reported that cinnamaldehyde improves adipose tissue function by reducing

visceral fat deposition, promoting lipolysis, fatty acid oxidation, and thermogenesis.<sup>13–15</sup> However, the cold-resistance effect of cinnamic acid remains to be further investigated. Glycyrrhiza is the dried root and rhizome of the *Glycyrrhiza uralensis*.<sup>16</sup> Its active components include licorice include polysaccharides, flavonoids, and triterpenoids. Studies have shown that glycyrrhiza flavonoids may play contribute to weight loss by promoting energy expenditure,<sup>17</sup> while the mechanism of the cold-resistance activity and its effect on the thermogenic protein levels in BAT remain unclear. Thus, this study aims to verify the thermogenic activity of GGD in a cold environment and explore its mechanism through network pharmacology analysis.

## Materials and methods

### Preparation of Guizhi Gancao decoction

According to the preparation recorded in "Treatise on Febrile Diseases", 7 kg of cinnamon (No. 180501, Bozhou Sanfeng Pharmaceutical Co Ltd., China) and 3.5 kg of licorice (No. 180901, Bozhou Sanfeng Pharmaceutical Co Ltd., China) were weighed and soaked in 10 times weight water for 30 min. The soaking liquid was decocted for 1.5 h in the TCM extraction tank. Then the filtered liquid residue was extracted again for 1 h. The filtrate was concentrated to 3200 mL (3700 g) in a low-temperature thickener, filtered through a No.3 sieve (0.355 mm), and stored the filtrate at  $-80^{\circ}\text{C}$ . After vacuum freeze-drying, each gram of dry powder GGD is equivalent to 11.835 g of crude herb. GGD liquid is dissolved in purified water. The positive control drug miglitol was purchased from Weiao Pharmaceuticals (Sichuan) Co., Ltd., China.

### Animals and administration

C57BL/6 J male mice were purchased from the animal center of the General Hospital of Northern Theater Command. Mice were randomly allocated into six groups ( $n = 10$ ), control (vehicle i.g without cold exposure), model (vehicle i.g with cold exposure after day 15th), Miglitol (50 mg/kg b.wt. per day with cold exposure after day 15th),<sup>9,18,19</sup> and GGD groups (1, 2, 4 g/kg b.wt. with cold exposure after day 15th) (Fig. 1A). The dose of GGD in the low-dose group (1 g/kg b.wt.) was equivalent to the adult's dose recorded in the ancient prescription. GGD was oral administered for 15 days before cold exposure. Mice in the control and model group were administered purified water. All mice were housed at room temperature with a 12-h light-dark cycle and fed chow and water *ad libitum*. Weight was recorded on alternate days.

### Cold exposure experiment

The dose of GGD in the low-dose group was equivalent to the daily dose of clinical adults recorded in the ancient prescription. A preliminary 14-day cold exposure experiment shows mice in the GGD group had significantly higher core body temperatures than the model group. Therefore, here we administrated GGD for 14 days continuously and implement acute cold exposure experiments on day 14th in  $-20^{\circ}\text{C}$  for 60 min. Then continue cold acclimation training in  $-20^{\circ}\text{C}$  for a week (30 min per day). On day 22nd, the cold-adapted mice were exposed to a cold experiment in  $-20^{\circ}\text{C}$  for 120 min and behavioral tests were taken. The experiment process *in vivo* is shown in Fig. 1B.

### Measurements of temperature

Rectal temperature (core body temperature) was measured with a mice thermometer before and after cold exposure. After the mice were fixed, the probe of the thermometer was gently inserted into the rectum for about 1.5 cm, and record the thermometer readings.<sup>20</sup> Mice were fasted 12 h before the experiment.<sup>21</sup> Surface

temperature was measured by a digital infrared camera (FLIR E5, FLIR Systems, Japan).

### Motor ability test of mice after cold exposure

Mice underwent running behavior training on day 16 and swimming behavior training on day 18. An electric shock applied at one end of the treadmill forced the mice to quickly run to the other side. The swimming training was conducted in a water maze, where the swimming distance in a 1.2-meter-diameter pool was recorded and measured using behavior recorder. After swimming, the mice were placed on a dry, fluffy pad to dry their fur. On day 21, the shortest time required for the mice to cross a 1-meter-long track at  $24^{\circ}\text{C}$  was recorded. Afterward, the mice were explored to  $-20^{\circ}\text{C}$  for 30 min following GGD administration. After 120 min of cold exposure at  $-20^{\circ}\text{C}$ , the shortest time for mice to cross the 1-meter track was recorded again. On day 22, the distance swum by the mice in the water maze tank within 1 min before administration was tracked using a small animal movement tracking system. After 30 min of oral administration, the mice were again explored to  $-20^{\circ}\text{C}$ . Following 120 min of cold exposure, the swimming distance for 1 min in the water maze tank was measured again. The motor ability of the mice was statistically analyzed before and after cold exposure. After the behavioral experiments, the mice were euthanized using an overdose of pentobarbital (150 mg/kg).

### The main components analysis in GGD by HPLC-Q-TOF-MS

For the chromatographic conditions, a Thermo-C18 column (4.6 mm  $\times$  250 mm, 5  $\mu\text{m}$ ) was used, and the mobile phase consisted of 0.1% formic acid aqueous solution (A) and acetonitrile (B). The gradient elution scheme is shown in Table 1. The flow rate was 0.6 mL/min, with a column temperature of  $25^{\circ}\text{C}$ . Detection wavelengths were 254 nm, 283 nm, and 360 nm, and the sample injection volume was 10  $\mu\text{L}$ . For the Mass spectrometry, an electrospray ionization source was used in negative ion scanning mode. The drying process was carried out at  $350^{\circ}\text{C}$  with a gas flow rate of 10 liters per minute, while the ion source temperature was maintained at  $320^{\circ}\text{C}$ . The atomization gas pressure was set to 40 psi, equivalent to 275.8 kPa (using the conversion factor of 1 psi = 6.895 kPa). Additionally, the capillary voltage was precisely regulated at 3500 V. The main components of GGD were identified by HPLC-Q-TOF-MS based on retention time,  $[\text{M}-\text{H}]^{-}$  molecular weight, and mass spectral intensity. The composition of the volatile oil from cinnamon was determined using positive ion MS. The molecular weight and SMILES structures of the compounds were searched in the Drug-Bank database (<https://www.drugbank.ca/>), leading to the inference of 49 major components.

### Network pharmacological analysis

The compound targets were collected from the STICH (<http://stitch.embl.de/>) and SwissTargetPrediction databases (<http://swisstargetprediction.ch/>), as well as relevant literature sources, specifically focusing on the main ingredients in GGD. Subsequently, a compound-target network was constructed in Cytoscape software (Version 3.7.2). Targets associated with thermogenesis and energy

**Table 1**  
HPLC gradient elution mode.

Time (min)	A (%)	B (%)
0	85	15
10	80	20
35	75	25
55	70	30
65	60	40
90	35	65

metabolism-related diseases were systematically retrieved from the DisGeNET and GeneCard databases, and the disease-target network was constructed. The overlapping targets identified within the two networks were designated as candidate targets to construction of both the compound-target-disease network and the protein-protein interaction (PPI) network. The PPI network was then leveraged to analyze key targets based on their degree values, with the corresponding compounds related to these targets being selected as key compounds. Furthermore, Gene Ontology Biological Process (GOBP) analysis and Kyoto Encyclopedia of Genes and Genomes (KEGG) analysis were performed on the candidate targets to speculate the pivotal biological processes and signaling pathways underlying the mechanisms of GGD.

#### Measurement of ATP production in BAT

Briefly, freshly extracted BATs from mice immediately post-cold exposure, excluding the blank control group, were homogenized using tissue lysis buffer. Moreover, the ATP concentration was measured by a commercial ATP Assay Kit (Catalog No. S0026; Beyotime) following manufacture's protocol.

#### Western blotting analysis

The protein of BAT was collected and homogenized in RIPA lysis buffer (Beyotime, P0013C), which was supplemented with protease inhibitor (Beyotime, P1005) and Phenylmethylsulfonyl fluoride (PMSF) (Beyotime, ST507), using a Dounce homogenizer. This homogenate was maintained on ice for 30 min, followed by centrifugation at 120,000 g for 15 min at 4°C. The supernatant was transferred to a new EP tube for protein quantification with BCA kit (Biosharp, BL521A), dilute all proteins to 2 µg/µL with SDS-PAGE sample loading buffer (Beyotime, P0015). These protein samples (30 µg) were loaded onto SDS-PAGE gels for separation, subsequently transferred onto polyvinylidene fluoride (PVDF) membranes, and then incubated overnight with 5% BSA at 4°C for effective blocking and sealing of the membranes. The corresponding primary antibodies (UCP1, Wanleibio, WL02625; PPAR $\gamma$ , Wanleibio, WL01800; PGC1- $\alpha$ , Wanleibio, WL02123; and  $\alpha$ -tubulin, Wanleibio, WL02296) and secondary antibodies (Proteintech, RGAR001; Proteintech, RGAM001) were incubated in sequence. Protein strips were developed and photographed, with protein expression levels quantitatively evaluated by gray analysis.

#### Statistical analysis

The experimental data were statistically analyzed using GraphPad Prism 9 (GraphPad Software, San Diego, CA, USA). One-way ANOVA or two-way ANOVA, along with the Turkey or Bonferroni method, were used for post-multiple comparisons. The experimental results were expressed as Mean  $\pm$  SEM, with  $p < 0.05$  indicating statistical significance. \* $p < 0.05$ , \*\* $p < 0.01$ , \*\*\* $p < 0.001$  vs. the control group; # $p < 0.05$ , ## $p < 0.01$ , ### $p < 0.001$  vs. the model group (Schematic diagram is shown in Fig. 2).

## Results

#### The thermogenic activity of GGD after cold exposure in mice

Acute cold exposure poses a life-threatening risk of hypothermia for individuals without cold adaptation. To investigate the thermogenic activity of GGD after 14 days of the administration, all groups except the blank control were subjected to 60 min acute exposure to  $-20^{\circ}\text{C}$  (Fig. 1A-B). Notably, the core body temperature of mice in the middle- and high-dose GGD groups was significantly higher than that of the model group during cold exposure. Moreover, infrared thermal images displayed a more extensive red area on the body surface of mice administered GGD, indicating a higher body surface temperature (Fig. 1C-D). This experiment proved that GGD significantly prevents the drop in

both core and surface temperatures caused by cold exposure, effectively maintaining body temperature in cold environment in a dose-dependent manner.

To more accurately mimic the conditions faced by people residing in cold regions during winter and explore the thermogenic activity of GGD on cold-adapted mice in a cold environment, mice were given daily 30-minute cold adaptation training at  $-20^{\circ}\text{C}$  from day 14–21 of drug administration. Subsequently, on day 22, a more severe 120-minute cold exposure test at  $-20^{\circ}\text{C}$  was conducted, with monitoring of both core body temperature and surface temperature. As shown in Fig. 1E-F, GGD, regardless of concentrations, significantly mitigated the drop in body surface temperature caused by cold exposure ( $p < 0.001$ ) compared to the cold exposure model group. These findings indicated that GGD could maintain both core and surface body temperature after cold adaptation.

#### Effect of GGD on the exercise ability and peripheral circulation of mice after cold exposure

In previous experiments, it was observed that the exercise capacity of mice decreased significantly with prolonged cold exposure, which is crucial for maintaining physical performance in cold environment.<sup>19</sup> To explore the difference in physical performance between groups exposed to cold, we recorded the time expended for mice to run across a 1-meter track and the swimming distance in a water maze pool over 1 min on the day 22 of administration, both before and after 120 min of cold exposure at  $-20^{\circ}\text{C}$ . As shown in Fig. 3A-B, after cold exposure, the running speed and swimming distance of the cold exposure model and miglitol group were significantly reduced compared to pre-cold exposure controls, indicating a notable limitation in their movement ability. While there was no significant difference in running ( $p > 0.05$ ) and swimming ability ( $p > 0.05$ ) before and after cold exposure in the GGD groups. In conclusion, compared to the cold exposure group, GGD can effectively maintain mice motor abilities under cold conditions.

After repeated cold exposure, mice in the cold-adapted group experienced tail swelling and necrosis due to disrupted peripheral circulation, vascular endothelial damage, and increased vascular permeability. These changes caused plasma extravasation and the release of inflammatory factors.<sup>19</sup> In this study, we explored the protective effect of GGD on peripheral circulation in a cold environment by measuring the length of non-necrotic tail segments across groups. As shown in Fig. 3C, both miglitol and GGD significantly alleviated cold-induced damage to extremities of mice in a dose-dependent manner. Notably, GGD at 1 g/kg b.wt. exhibited a protective effect similar to miglitol, whereas GGD at 4 g/kg b.wt. provided the greatest protective effect.

#### Identification of the main components of GGD

HPLC-Q-TOF-MS analysis chromatogram of GGD is shown in Fig. 4. The total ion flow in negative ion mode is presented in Fig. 4A, while the chromatograms at detection wavelengths of 254 nm and 283 nm are displayed in Fig. 4B-C, respectively. Based on the molecular ion peak [M-H]<sup>-</sup> molecular weight analysis from mass spectrometry, 49 compounds were identified by comparing with literature (Supplementary table 1). GGD contains numerous flavonoids and triterpenoids in GGD, which have been confirmed to play a role in regulating energy metabolism.<sup>22–25</sup>

#### The thermogenic effect of GGD analyzed by network pharmacology

First, we constructed a Compound-Target network. By searching Swiss Target Prediction and STITCH databases, 114 targets of 24 compounds in GGD were screened out, and 29 pairs of compound-target relationships were added according to the literature. Additional targets and references are shown in Table 2. A total of 24 compounds and 128

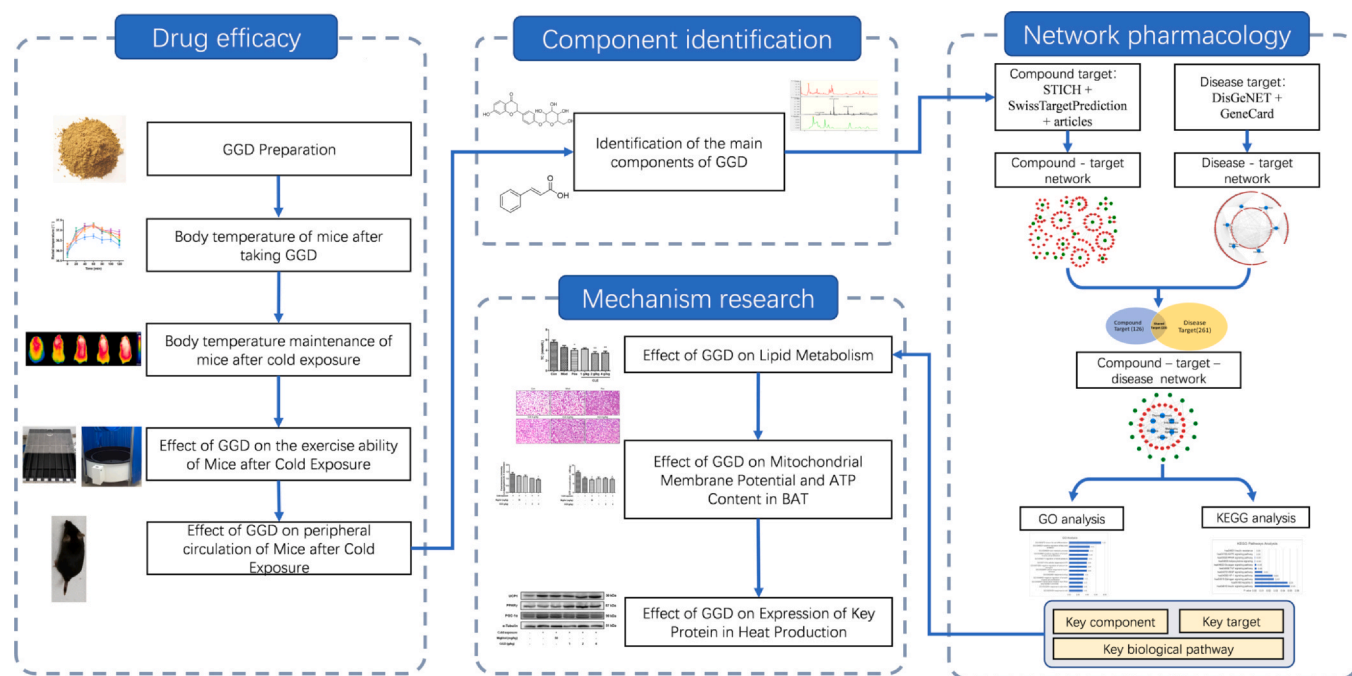


Fig. 2. Schematic diagram.

targets were imported into Cytoscape software to construct a compound-target network (Fig. 5A). According to the network degree analysis, catechuic acid, glycyrrhiza A, afzelin, cinnamic acid, glycyrrhiza chalcone D, etc., may play crucial roles in the thermogenic effect of GGD. Additionally, AKR1 $\beta$ , CEBP $\alpha$ , PPAR $\gamma$ , etc., emerged as the key targets (Table 3).

Second, a disease-target network was constructed. The genes related to thermogenesis, obesity, cold intolerance, metabolic

syndrome, type 2 diabetes, and cold were searched in DisGeNET and GeneCard databases. After screening, 261 disease-related targets and 379 correlation pairs were identified. Disease-target information was input into Cytoscape software to create the disease-target network for GGD (Fig. 5B). Based on the disease-target network analysis, UCP1, PPAR $\gamma$ , and PGC1- $\alpha$  were identified as potential key targets for the cold-resistant effects of GGD (Table 4), though further analysis and validation were required.

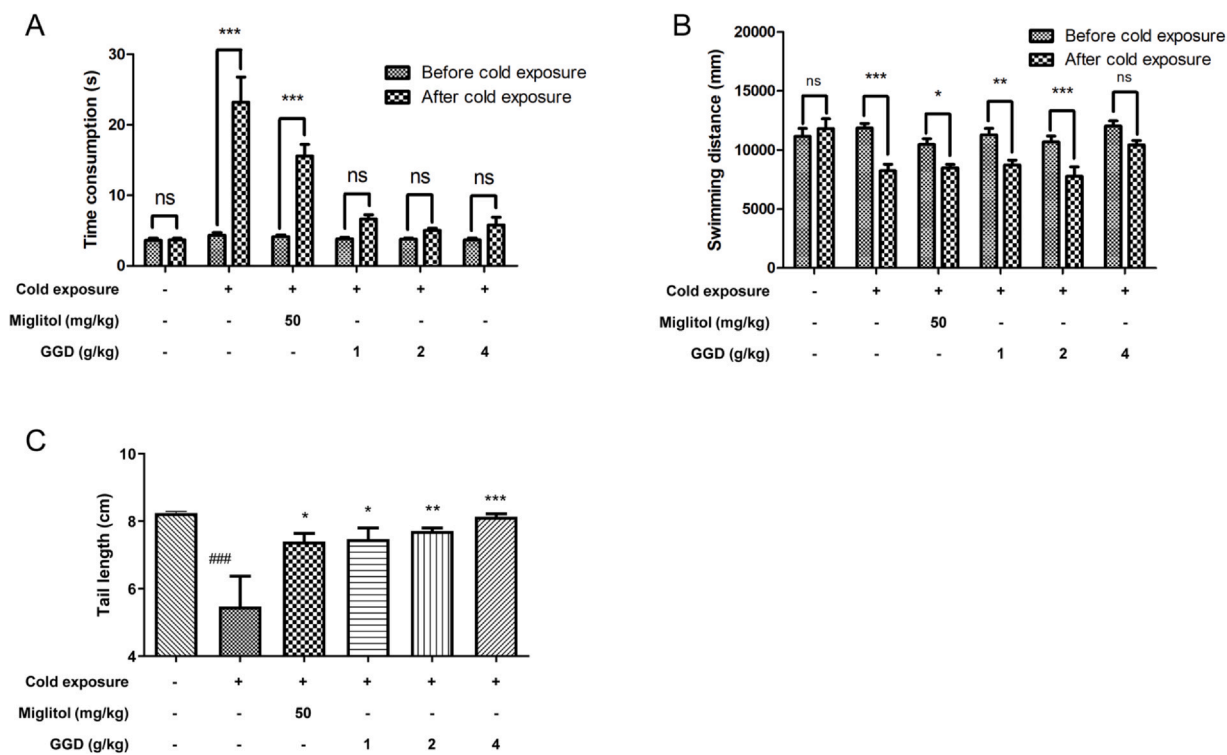
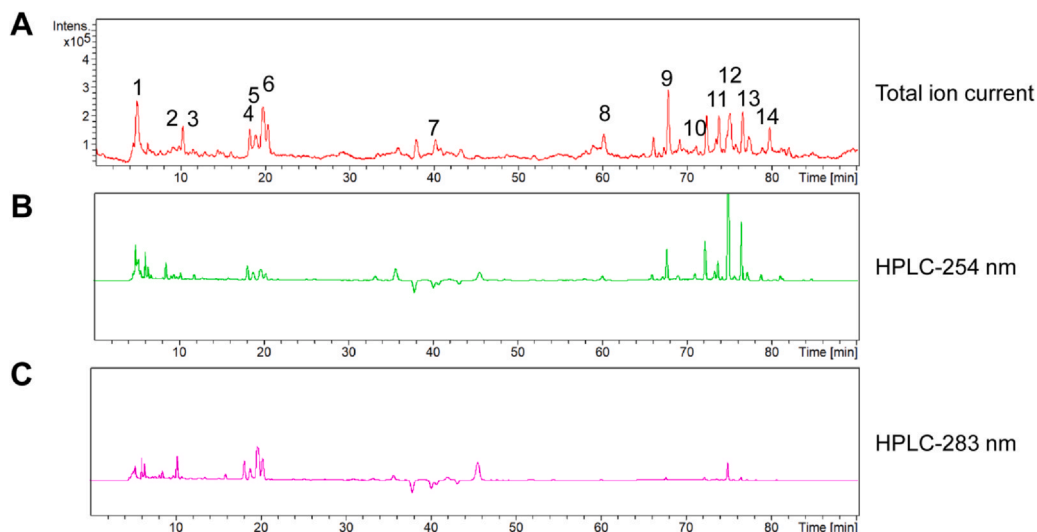


Fig. 3. GGD could maintain the athletic ability and peripheral circulation in a cold environment. (A) The time mice took to cross a 1 m-long track. (B) The distance mice swim for 1 min. (C) The tail lengths of mice after frequency cold exposure Data were presented as mean  $\pm$  SEM by two-way repeated measure ANOVA and Bonferroni post-tests. N = 7–9, \* p < 0.05, \*\* p < 0.01, and \*\*\* p < 0.001 vs. the time cost or distance before cold exposure or compared with Model group.



**Fig. 4.** HPLC-Q-TOF-MS analysis. (A) The total negative ion current of GGD. (B, C) The HPLC image detected at 254 nm, 283 nm.

Third, we constructed and analyzed the compound-target-disease network. According to the common targets between the compound-disease network and disease-target network, we developed the compound-target-disease network (Fig. 5C-D) and PPI network (Fig. 5E), with the latter constructed using STRING (Fig. 5F). According to the degree values in the Protein-protein interaction network (PPI) network, PPAR $\gamma$ , PGC1- $\alpha$ , and UCP1 may be the key targets contributing to the cold resistance properties of GGD.

Next, GOBP analysis and KEGG analysis were performed. The targets from the compound-target-disease network were input into the David database, and the top 13 biological processes were identified based on  $-\log_{10}$  P values (Fig. 5G-I). These results suggested that the key biological processes through which GGD exerts its thermogenic effect in a cold environment induced promoting brown fat differentiation, fatty acid oxidation, and lipid metabolism. The targets in the compound-target-disease network were then imported into the KEGG database, where 9 key signaling pathways were screened out based on P values. Among these, the thermogenic and PPAR pathway may be critical for GGD's role in promoting fatty acid oxidation and lipid metabolism, thereby increasing heat production and enhancing cold resistance.

#### Effect of GGD on lipid metabolism in mice

Thermogenic regulation is often accompanied by changes in energy metabolism. To explore the effect of GGD on lipid metabolism, biochemical indexes of serum collected after cold exposure were tested. As shown in Fig. 6A-B, total cholesterol (TC) was significantly reduced in the cold exposure model group compared to the blank control group ( $p < 0.01$ ). Furthermore, the TC levels were significantly lower in the miglitol group ( $p < 0.05$ ) compared with the cold exposure group, with an even more pronounced reduction observed in medium- and high-dose GGD group ( $p < 0.01$ ). However, no significant differences in total triglyceride (TG) levels were found among all groups. In

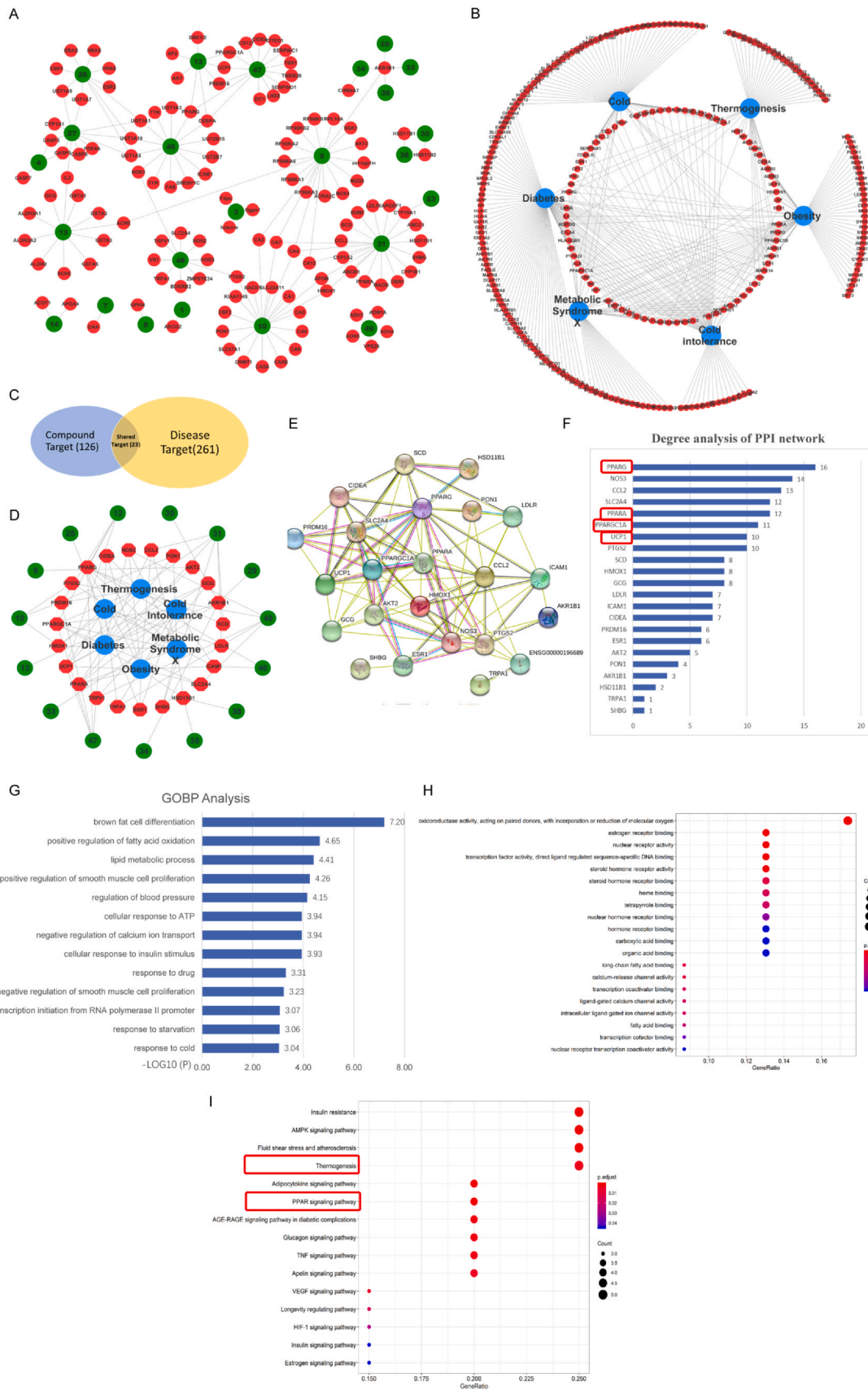
mammals, BAT is activated by cold or drug stimulation, leading to a reduction in adipocyte size and fat droplet volume, resulting in a multicellular morphology that provides substrates for mitochondrial thermogenesis. As shown in Fig. 6C, the cold exposure model group displayed a decrease in brown adipose cell and fat droplet volume compared to the blank control group, suggesting that cold exposure promotes BAT activation and thermogenesis. Lipid droplet volume significantly decreased in the miglitol group, and a similar reduction was observed in the medium- and high-dose GGD groups, where BAT exhibited a more pronounced multicellular morphology, facilitating fat mobilization and utilization. These results demonstrate that GGD reduces serum total cholesterol levels, promoted the BAT activation, and accelerated metabolism, ultimately contributing to increased heat production.

#### Effect of GGD on mitochondrial membrane potential and ATP content in BAT

In the proton leakage hypothesis, the mitochondrial membrane potential associated with thermogenesis is reduced, resulting in the uncoupling of oxidative phosphorylation and the transformation of energy to heat without ATP production.<sup>31</sup> To investigate the effect of GGD on the mitochondrial membrane potential of BAT, the total mitochondria were purified and isolated from fresh tissue samples obtained after cold exposure, and the mitochondrial membrane potential test was performed by the JC-1 detection kit. As shown in Fig. 6D, the red fluorescence intensity of mitochondria in the blank control group and the cold exposure model group was stronger, while the green fluorescence intensity was weaker, demonstrating a significant difference between these two groups ( $p < 0.05$ ). While there was no significant difference in the intensity of red fluorescence and green fluorescence in BAT mitochondria of mice treated with GGD. The ratio of red to green fluorescence was shown in Fig. 6E. Compared with the cold exposure model group, the BAT mitochondrial membrane potential

**Table 2**  
Complementary targets from articles.

Compound number	Compound name	Target	Reference
31	Liquiritigenin	AMPK, ACC	26
15	Licoisoflavanone	ACOT1, APOA4	27
12	Licochalcone D	UCP1, PRDM16, PGC, ERK1/2, AKT, PPARG, AP2, CEBPA	28,29
47	Cinnamic acid	UCP1, PRDM16, PGC, CIDEA, PPARG, PRDM16, CEBPA	29
46	Hispaglabridin A	SREBP1C, PPARG, FAS	30



(caption on next page)

**Fig. 5.** The thermogenic mechanism of GGD analyzed by network pharmacology. (A) Compound-target interaction network. The green nodes represent the constituent compounds contained in GGD; the red nodes represent the associated protein targets. (B) Target-disease interaction network. The blue nodes represent the diseases related to thermogenesis; the red nodes represent the associated proteins of targets. (C-F) Compound-target-disease network analysis. (C) Shared targets in the Compound-target interaction network and the Target-disease interaction network. (D) Compound-target-disease interaction network. The green nodes represent the constituent compounds contained in GGD; the blue nodes represent the diseases related to thermogenesis; the red nodes represent the associated proteins of targets. (E) Protein-protein interaction (PPI) network made by STRING. (F) Degree analysis of PPI network. (G-H) Gene ontology biological process analyzed by DAVID. (I) Key KEGG pathways.

**Table 3**

Key compounds and key targets in the compound-target interaction network.

Compound	Degree	Target	Degree
Catechin	20	AKR1B1	5
Liquiritigenin	20	CEBPA	3
Afzelin	19	PPARG	3
Hispaglabridin A	14	CA12	3
Cinnamic acid	14	CA4	3
Ononin	11	CA7	3
Formononetin	11	UGT1A1	3
Cinnamaldehyde	10	UGT1A10	3
Coumestrol	10	UGT1A8	3
Licochalcone D	8	PPARGC1A	2
Cinnamyl alcohol	5	PRDM16	2
Gancaonin N	3	UCP1	2
Gancaonin B	3		

**Table 4**

Key targets in the target-disease interaction network.

Disease	Degree	Target	Degree
Diabetes	101	UCP1	6
Obesity	71	PPARG	5
Cold	70	PPARGC1A	5
Cold Intolerance	53	INS	5
Thermogenesis	44	ADIPOQ	5
Metabolic Syndrome X	40	IL6	5
		PPARA	5

in the high-dose GGD group (4 g/kg b.wt.) was significantly lower ( $p < 0.05$ ). These results indicated that GGD could decrease the mitochondrial membrane potential of BAT in cold-exposed mice.

In the proton leakage hypothesis, the reduction of mitochondrial membrane potential leads to the uncoupling of oxidative phosphorylation, resulting in a decrease in intracellular ATP production. To investigate the potential thermogenic mechanism of GGD, the ATP content in BAT was detected. As shown in Fig. 6F, although ATP content was lower in the cold exposure model group compared to the blank control group, this difference was not statistically significant ( $p \geq 0.05$ ). However, both the miglitol and the high-dose GGD group (4 g/kg b.wt.) could significantly reduce the ATP content in BAT ( $p < 0.05$ ). These results indicated that GGD could promote the uncoupling of the mitochondrial oxidative respiratory chain by reducing mitochondrial membrane potential and ATP generation, and promote the conversion of energy into heat, thus exerting the thermogenic effect.

#### Effect of GGD on expression of key protein in heat production

The network pharmacological analysis indicated that the key targets for the thermogenic effect of GGD were UCP1, PPAR $\gamma$ , PGC1- $\alpha$ , etc., so the expression levels of key heat-producing proteins in BAT of mice were verified by Western-blot. UCP1 is a key protein involved in the uncoupling of the respiratory chain in mitochondria and plays a role in heat generation.<sup>32</sup> PPAR $\gamma$  and PGC1- $\alpha$  are upstream proteins of UCP1, which are responsible for regulating the expression of protein pathways in energy metabolism.<sup>33</sup> The protein expressions of UCP1, PPAR $\gamma$ , and PGC1- $\alpha$  in BAT were shown in Fig. 6G-J. The protein expression of

UCP1 was significantly increased after cold adaptation across different treatment groups, especially in the high-dose GGD group. PPAR $\gamma$  levels in the BAT of GGD-treated mice was significantly higher than that in the cold exposure model group ( $p < 0.01$ ) in a dose-dependent manner. The expression levels of PGC1- $\alpha$  in BAT of medium-dose and high-dose GGD groups were significantly higher than those of the blank control group, but there was no significant difference compared to the cold exposure model group. Overall, these results suggested that GGD could promote intracellular fat mobilization and utilization by upregulating PPAR $\gamma$  and its downstream protein UCP1 in BAT, thereby enhancing thermogenesis through mitochondrial respiratory chain uncoupling.

#### Discussion

As one of the most renowned classical formulas in TCM, GGD exemplifies Zhang Zhongjing's theory of Xin Gan Hua Yang (pungent and sweet flavors transforming into Yang). This theory refers to the compatibility of a pungent-flavored herb with a sweet-flavored herb to generate and invigorate Yang Qi.<sup>34</sup> Here, Yang and Qi denote the essential Qi of organs, serving as the material foundation of human vital activities and the driving force for bodily functions.<sup>35</sup> In modern medicine, the concept of "energy" aligns with this interpretation, as energy is recognized as the impetus of life. Mitochondria are responsible for over 95% of bodily energy production and play a pivotal role in sustaining life and vitality. Thus, the TCM concept of Yang Qi can be analogized to "energy" in modern medicine, providing a theoretical basis for investigating the effects of GGD on energy metabolism.

The thermogenic function of BAT is based on the uncoupling of oxidative phosphorylation from ATP production, an evolutionary mechanism for thermoregulation during cold exposure.<sup>36</sup> UCP1, a key regulator of cold-induced thermogenesis, plays an irreplaceable role in this uncoupling process.<sup>3</sup> UCP1 is localized on the inner mitochondrial membrane of brown adipocytes. Studies have demonstrated that *Ucp1*-knockout mice fail to maintain core body temperature and develop hypothermia upon acute cold exposure.<sup>37</sup> The catabolism of fatty acids and glucose provides energetic substrates for the thermogenic process.<sup>38</sup> Although the reduction in mitochondrial membrane potential may affect mitochondrial function, it does not necessarily impair mitochondrial activity, owing to the self-repairing and adaptive capacities of mitochondria.<sup>39</sup>

As a TCM preparation, GGD exhibits distinct advantages over single-agent UCP1 activators (e.g., miglitol) and individual herbal components (cinnamon/glycyrrhiza). CL-316,243 is a well-recognized UCP1 agonist that effectively preserves core body temperature in cold environments. However, its potent uncoupling activity may induce hyperthermia, energy imbalance, metabolic disorders, and even cellular necrosis and organ damage. Among clinically approved drugs, retinoids have been verified to activate UCP1 efficiently,<sup>40-42</sup> whereas these compounds are associated with adverse effects such as retinoic acid syndrome, which can be fatal in severe cases.<sup>43</sup> In addition, miglitol and other antidiabetic agents have been reported to upregulate UCP1 expression in mice fed a high-fat diet.<sup>8,9</sup> In the present study, miglitol was used as the positive control; nevertheless, it elicits prominent gastrointestinal adverse reactions including flatulence, diarrhea, nausea, and vomiting.<sup>44</sup> Our findings demonstrated that GGD has a higher UCP1 activation efficiency than miglitol, exerts a milder influence on exercise capacity following cold exposure, and exhibits favorable safety profiles.

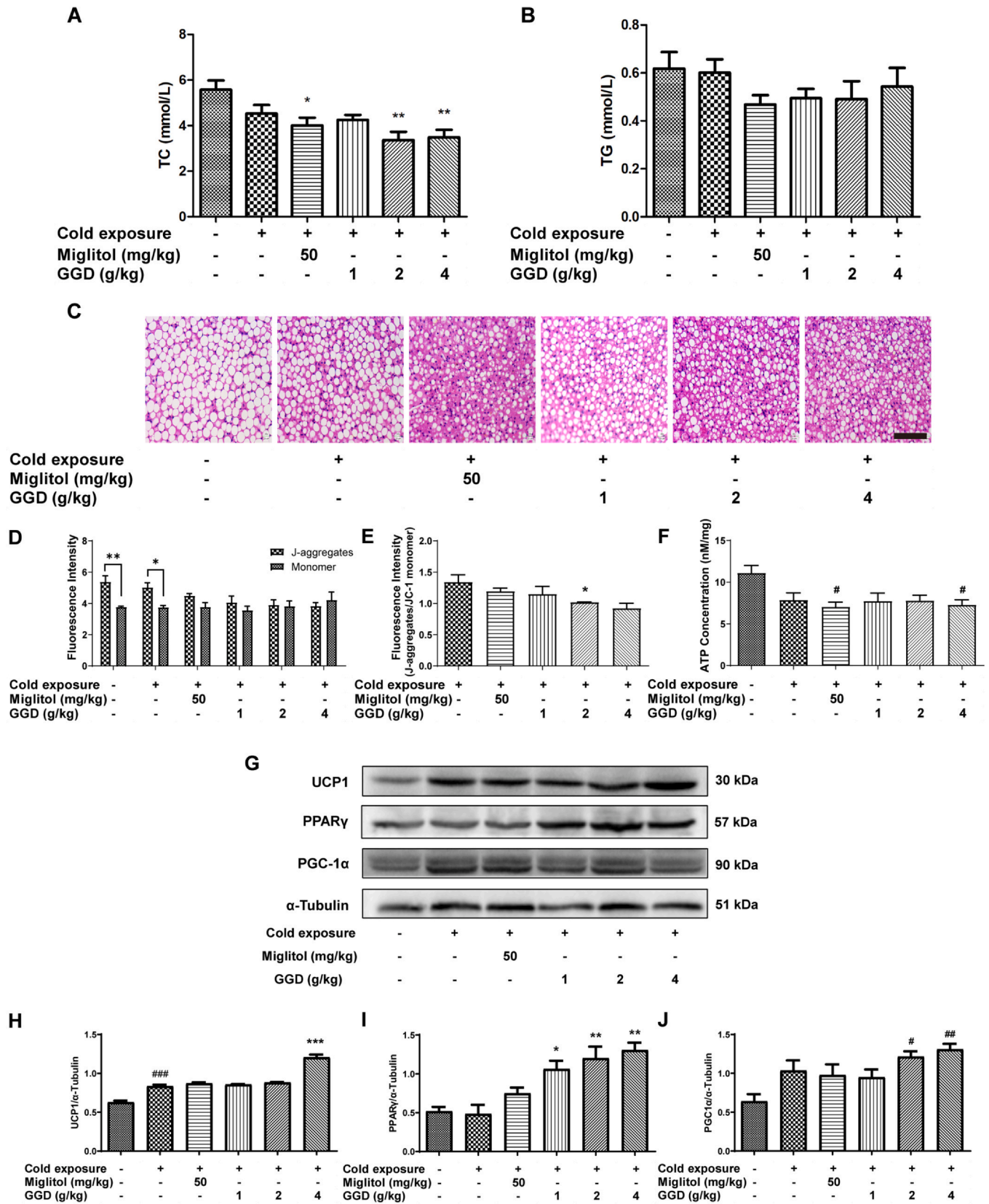


**Fig. 6.** Mechanism verification of GGD thermogenesis. (A) Serum total cholesterol (TC). (B) Serum total triglyceride (TG). (C) H&E staining of BAT after GGD drug intake and cold exposure in C57 mice. Sections were 100  $\mu$ m thick and photomicrographs were taken at 400  $\times$ . (D) Fluorescence intensity of JC-1 aggregates and JC-1 Monomer. \* $p$  < 0.05, \*\* $p$  < 0.01 difference between JC-1 aggregates and JC-1 Monomer fluorescence intensity. (E) The ratio of fluorescence intensity of JC-1 aggregates and JC-1 Monomer. Data were analyzed by one-way ANOVA and Dunnett's Multiple Comparison Test. \* $p$  < 0.05 vs. Cold exposure group. (F) ATP concentration in mice BAT. Data were analyzed by one-way ANOVA and Tukey's Multiple Comparison Test ( $n$  = 3). (G) Western blot of UCP1, PPAR $\gamma$ , PGC-1, and  $\alpha$ -tubulin in mice BAT. (H-J) Quantification of relative changes in UCP1, PPAR $\gamma$ , PGC-1 expression relative to  $\alpha$ -Tubulin. Data are presented as mean  $\pm$  SEM,  $n$  = 9 (A-C) or 3 (C-J). #  $p$  < 0.05, ##  $p$  < 0.01, ###  $p$  < 0.001 vs. control group. \*  $p$  < 0.05, \*\*  $p$  < 0.01, \*\*\*  $p$  < 0.001 vs. model group.

In terms of the mechanism, PPAR $\gamma$ , a nuclear receptor, acts as a key transcription factor regulating adipose tissue function and plays a critical role in thermoregulation.<sup>33,45,46</sup> PGC1- $\alpha$ , a nuclear receptor coactivator of PPAR $\gamma$ , interacts with transcription factors to stimulate mitochondrial biogenesis, enhance respiration, and improve mitochondrial efficiency.<sup>47</sup> PGC1- $\alpha$  serves as an essential regulator in the thermogenic pathway of BAT and regulates several thermogenic factors.<sup>33,47,48</sup> In mice, *Pgc1*-knockout impaired adaptive thermogenesis regulation during cold stimulation.<sup>46</sup> PGC1- $\alpha$  is the target gene of PPAR $\gamma$ , and enhances the transcriptional activity of PPAR $\gamma$  through coactivation, which in turn increases its own expression and promotes the expression of PPAR $\gamma$  target genes. This creates a positive feedback loop that amplifies the effects of both.<sup>33</sup> Based on network pharmacological analysis, the potential thermogenic effect of GGD under cold stimulation may be associated with elevated biological activities and protein expression of PPAR $\gamma$  and PGC1- $\alpha$ , and subsequent activation of downstream thermogenic pathway, though further validation is required.

This study has several limitations: (1) The acute and chronic cold exposure mouse models employed herein may not fully recapitulate the process of long-term cold adaptation in humans. (2) Given the complexity of traditional Chinese medicine components, although 49 ingredients were identified, no further refined experiments were conducted to verify the necessity of individual components, and the mechanism underlying the synergistic effect requires more in-depth elucidation. (3) Regarding clinical translation, since the oral bioavailability of GGD and the activation threshold of human BAT have not been evaluated, subsequent studies should further validate these aspects using techniques such as PET-CT.

In summary, this study investigated the anticold effect of GGD. The potential mechanism underlying its anticold activity was predicted via component identification and network pharmacology, and subsequently validated by molecular biology approaches to clarify the biological pathways and key targets. These findings provide a novel theoretical basis for the development of TCM-based anticold agents. The conclusions are as follows: (1) Regarding the anticold effect, GGD can effectively maintain core body temperature, surface temperature, and exercise capacity in mice under cold conditions, while protecting extremity tissues, which is attributed to its ability to enhance systemic thermogenesis. (2) In terms of the anticold mechanism, under cold stimulation, key compounds in GGD (including licochalcone D, glabridin, and cinnamic acid) reduce lipid droplet volume and improve lipid metabolism in mouse BAT, thereby providing substrates for mitochondrial energy metabolism. Furthermore, GGD upregulates the expression of UCP1 and its upstream proteins PPAR $\gamma$  and PGC1- $\alpha$  in BAT, decreases mitochondrial membrane potential, and reduces ATP production. This uncouples energy production from ATP synthesis, leading to energy dissipation in the form of heat and enhanced thermogenesis, which ultimately exerts the anticold effect. Collectively, it lays a new theoretical foundation for the development of TCM thermogenic agents for cold regions.

## Conclusion

GGD exhibits significant potential in enhancing thermogenesis and cold resistance. By boosting heat production and protecting peripheral circulation, GGD effectively maintains core body temperature, surface temperature, and motor ability in mice exposed to cold environments. Key compounds in GGD, such as glycyrrhiza chalcone D, glycyrrhiza A, and cinnamic acid, are predicted to enhance lipid metabolism by reducing lipid droplet volume in brown adipose tissue, thereby fueling mitochondrial energy metabolism. Additionally, GGD increases the expression of UCP1 and its upstream regulator PPAR $\gamma$  in BAT. This upregulation culminates in a cascade of events, including the attenuation of mitochondrial membrane potential, decreased ATP production, and a concomitant surge in heat generation. These combined effects contribute significantly to GGD's cold resistance properties. These

findings suggest that GGD has the potential to be developed as a therapeutic agent for enhancing cold resistance. Further investigations are required to validate these mechanisms in humans and to ensure the safety and efficacy of GGD in clinical settings.

## Declarations

Not applicable.

## CRediT authorship contribution statement

**Zexu Shen:** Writing – original draft, Validation, Data curation. **Xiang Li:** Methodology, Conceptualization. **Chenghui Yan:** Methodology, Conceptualization. **Tianshu Ren:** Methodology. **Bo Xing:** Methodology. **Yingying Qu:** Formal analysis. **Dong Yao:** Data curation. **Zihua Xu:** Writing – review & editing, Supervision. **Yaling Han:** Writing – original draft, Resources. **Qingchun Zhao:** Writing – review & editing, Supervision, Project administration, Methodology, Conceptualization.

## Ethics approval and consent to participate

We minimized the number of animals used and all experiments were considered to reduce animal suffering. All procedures involving animals were in accordance with the ethical standards of the Committee on the Ethics of Animal Experiments of the General Hospital of Northern Theater Command (NO. 2023-54, NO. 2025-21).

## Consent for publication

This work is original and has not been published nor is it currently under consideration for publication elsewhere. All authors have read and approved the final manuscript. We consent to the publication of this manuscript in Precision Medication and agree to transfer copyright to the publisher. Any materials reproduced from other sources are properly licensed or fall under fair use.

## Availability of data and materials

All experimental materials are available from the corresponding author upon reasonable request.

## Funding

Not applicable.

## Declaration of Competing interest

The authors declare that they have no known competing financial interests or personal relationships that could have appeared to influence the work reported in this paper.

## Acknowledgements

Not applicable.

## Authors' other information

Not applicable.

## Appendix A. Supporting information

Supplementary data associated with this article can be found in the online version at [doi:10.1016/j.pmedi.2026.100077](https://doi.org/10.1016/j.pmedi.2026.100077).

## References

- Conlon KC, Rajkovich NB, White-Newsome JL, Larsen L, O'Neill MS. Preventing cold-related morbidity and mortality in a changing climate. *Maturitas*. 2011;69(3):197–202.
- O'Donnell FL, Stahlman S, Oetting AA. Update: cold weather injuries, active and reserve components, U.S. Armed Forces, July 2012–June 2017. *Msmr*. 2017;24(10):12–21.
- Cannon B, Nedergaard J. Brown adipose tissue: function and physiological significance. *Physiol Rev*. 2004;84:277–359.
- Hart J. Effects of temperature and work on metabolism, body temperature, and insulation: results with mice. *Can J Zool*. 1952;30(1):90–98.
- Foster DO. Quantitative contribution of brown adipose tissue thermogenesis to overall metabolism. *Can J Biochem Cell Biol*. 1984;62(7):618–622.
- Garcia C, Vannostrand D, Majd M, et al. Benzodiazepine-resistant "brown fat" pattern in positron emission tomography: two case reports of resolution with temperature control. *Mol Imaging & Biol*. 2004;6(6):368–372.
- Clarke KJ, Porter RK. Uncoupling protein 1 dependent reactive oxygen species production by thymus mitochondria. *Int J Biochem & Cell Biol*. 2013;45(1):81–89.
- Sasaki T, Hiraga H, Yokotahashimoto H, Kitamura T. Miglitol protects against age-dependent weight gain in mice: a potential role of increased UCP1 content in brown adipose tissue [Rapid Communication]. *Endocr J*. 2015;62(5):469–473.
- Sugimoto S, Nakajima H, Kodo K, et al. Miglitol increases energy expenditure by upregulating uncoupling protein 1 of brown adipose tissue and reduces obesity in dietary-induced obese mice. *Nutr & Metab*. 2014;11(1):1–11.
- Ko KM, Mak DH, Chiu PY, Poon MK. Pharmacological basis of 'Yang-invigoration' in Chinese medicine. *Trends Pharm Sci*. 2004;25(1):3–6.
- Wang XM, Li XB, Peng Y. Impact of Qi-invigorating traditional Chinese medicines on intestinal flora: a basis for rational choice of prebiotics. *Chin J Nat Med*. 2017;15(4):241–254.
- Wang P, Chi J, Guo H, et al. Identification of differential compositions of aqueous extracts of cinnamomi ramulus and cinnamomi cortex. *Molecules*. 2023;28(5):2015.
- Watanabe T, Terada Y. Food Compounds Activating Thermosensitive TRP Channels in Asian Herbal and Medicinal Foods. *J Nutr Sci Vitaminol*. 2015;61(Suppl):S86–S88.
- Khare P, Jagtap S, Jain Y, Baboota RK, Bishnoi M. Cinnamaldehyde supplementation prevents fasting-induced hyperphagia, lipid accumulation, and inflammation in high-fat diet-fed mice. *BioFactors*. 2016;42(2):201–211.
- Tamura Y, Iwasaki Y, Narukawa M, Watanabe T. Ingestion of cinnamaldehyde, a TRPA1 agonist, reduces visceral fats in mice fed a high-fat and high-sucrose diet. *J Nutr Sci Vitaminol*. 2012;58(1):9–13.
- Commission CP. *Pharmacopoeia of the People's Republic of China*. People's Medical Publishing House; 2005.
- Lee J, Choe SS, Jang H, et al. AMPK activation with glabridin ameliorates adiposity and lipid dysregulation in obesity. *J Lipid Res*. 2012;53(7):1277–1286.
- Zu Y-x, Lu H-y, Liu W-w, et al. Jiang Gui Fang activated interscapular brown adipose tissue and induced epididymal white adipose tissue browning through the PPAR $\gamma$ /SIRT1-PGC1 $\alpha$  pathway. *J Ethnopharmacol*. 2020;248:112271.
- Liu X, Gao Y-p, Shen Z-x, et al. Study on the experimental verification and regulatory mechanism of Rougui-Ganjiang herb-pair for the actions of thermogenesis in brown adipose tissue based on network pharmacology. *J Ethnopharmacol*. 2021;114378.
- Pandit C, Sai Latha S, Usha Rani T, Anilakumar KR. Pepper and cinnamon improve cold induced cognitive impairment via increasing non-shivering thermogenesis; a study. *Int J Hyperth*. 2018;35:518–527.
- Wang N, Lu H, Li X, Du Y, Zhao Q. ZW290 increases cold tolerance by inducing thermogenesis via the upregulation of uncoupling protein 1 in brown adipose tissue in vitro and in vivo. *Lipids*. 2019;54(5):265–276.
- Cassidy A, Minihane AM. The role of metabolism (and the microbiome) in defining the clinical efficacy of dietary flavonoids. *Am J Clin Nutr*. 2017;105(1):10–22.
- Mozaffarian D, Wu JHY. Flavonoids, dairy foods, and cardiovascular and metabolic health: a review of emerging biologic pathways. *Circ Res*. 2018;122(2):369–384.
- Bai L, Li X, He L, et al. Antidiabetic potential of flavonoids from traditional Chinese medicine: a review. *Am J Chin Med*. 2019;47(5):933–957.
- Mamouni K, Kallifatidis G, Lokeshwar BL. Targeting mitochondrial metabolism in prostate cancer with triterpenoids. *Int J Mol Sci*. 2021;22(5).
- Lee JW, Choe SS, Jang H, et al. AMPK activation with glabridin ameliorates adiposity and lipid dysregulation in obesity. *J Lipid Res*. 2012;53(7):1277–1286.
- Aoki F, Honda S, Kishida H, et al. Suppression by licorice [*Glycyrrhiza glabra*] flavonoids of abdominal fat accumulation and body weight gain in high-fat diet-induced obese C57BL/6J mice. *Biosci Biotechnol & Biochem*. 2007;71(1):206–214.
- Eun LH, Gabsik Y, Sin-Hee H, et al. Anti-obesity potential of *Glycyrrhiza uralensis* and licochalcone A through induction of adipocyte browning. *Biochem & Biophys Res Commun*. 2018;503(3):2117–2123.
- Hong GP, Bak EJ, Woo GH, et al. Licochalcone E has an antidiabetic effect. *J Nutr Biochem*. 2012;23(7):759–767.
- Ahn J, Lee H, Jang J, Kim S, Ha T. Anti-obesity effects of glabridin-rich supercritical carbon dioxide extract of licorice in high-fat-fed obese mice. *Food & Chem Toxicol*. 2013;51(Complete):439–445.
- Bertholet AM, Chouchani ET, Kazak L, et al. H(+) transport is an integral function of the mitochondrial ADP/ATP carrier. *Nature*. 2019;571(7766):515–520.
- Fedorenko A, Lishko PV, Kirichok Y. Mechanism of fatty-acid-dependent UCP1 uncoupling in brown fat mitochondria. *Cell*. 2012;151(2):400–413.
- Boström P, Wu J, Jedrychowski MP, et al. A PGC1- $\alpha$ -dependent myokine that drives brown-fat-like development of white fat and thermogenesis. *Nature*. 2012;481(7382):463–468.
- Lv Y, Gao J. "Warming yang with pungent and sweet nature" compatibility of Guizhiganciao Decoction. *Zhong Yao Cai*. 2010;33(8):1296–1299.
- Leong PK, Wong HS, Chen J, Ko KM. Yang/Qi invigoration: an herbal therapy for chronic fatigue syndrome with yang deficiency? *Evid Based Complement Altern Med*. 2015;2015:945901.
- Kozak LP. Brown fat and the myth of diet-induced thermogenesis. *Cell Metab*. 2010;11(4):263–267.
- Feldmann HM, Golozoubova V, Cannon B, Nedergaard J. UCP1 ablation induces obesity and abolishes diet-induced thermogenesis in mice exempt from thermal stress by living at thermoneutrality. *Cell Metab*. 2009;9(2):203–209.
- Lowell BB, Spiegelman BM. Towards a molecular understanding of adaptive thermogenesis. *Nature*. 2000;404(6778):652–660.
- Singh R, Barrios A, Dirakvand G, Pervin S. Human brown adipose tissue and metabolic health: potential for therapeutic avenues. 2021;10(11):3030.
- Murholm M, Isidor MS, Basse AL, et al. Retinoic acid has different effects on UCP1 expression in mouse and human adipocytes. *BMC Cell Biol*. 2013;14(1):41.
- Rial E, Gonzalezbarroso MM, Fleury C, et al. Retinoids activate proton transport by the uncoupling proteins UCP1 and UCP2. *EMBO J*. 1999;18(21):5827–5833.
- Shabalina IG, Backlund EC, Bartana J, Cannon B, Nedergaard J. Within brown-fat cells, UCP1-mediated fatty acid-induced uncoupling is independent of fatty acid metabolism. *Biochim Et Biophys Acta*. 2008;1777(7):642–650.
- Tallman MS, Andersen JW, Schiffer CA, Appelbaum FR, Wiernik PH. Clinical description of 44 patients with acute promyelocytic leukemia who developed the retinoic acid syndrome. *Blood*. 2000;95(1):90–95.
- Scott LJ, Spencer CM. Miglitol: a review of its therapeutic potential in type 2 diabetes mellitus. *Drugs*. 2000;59(3):521–549.
- Tan HL, Guan XH, Hu M, et al. Human amniotic mesenchymal stem cells-conditioned medium protects mice from high-fat diet-induced obesity. *Stem Cell Res & Ther*. 2021;12(1):364.
- Festuccia WT, Blanchard PG, Oliveira TB, Magdalon J, Deshaies Y. PPAR activation attenuates cold-induced upregulation of thyroid status and brown adipose tissue PGC-1 and D2. *Am J Physiol Regul Integr & Comp Physiol*. 2012;303(12):R1277.
- Finck BN, Kelly DP. PGC-1 coactivators: inducible regulators of energy metabolism in health and disease. *J Clin Investig*. 2006;116(3):615–622.
- Zhang Z, Zhang H, Li B, et al. Berberine activates thermogenesis in white and brown adipose tissue. *Nat Commun*. 2014;5:5493.